Journal of Materials Chemistry

www.rsc.org/materials

Volume 21 | Number 43 | 21 November 2011 | Pages 17009–17548

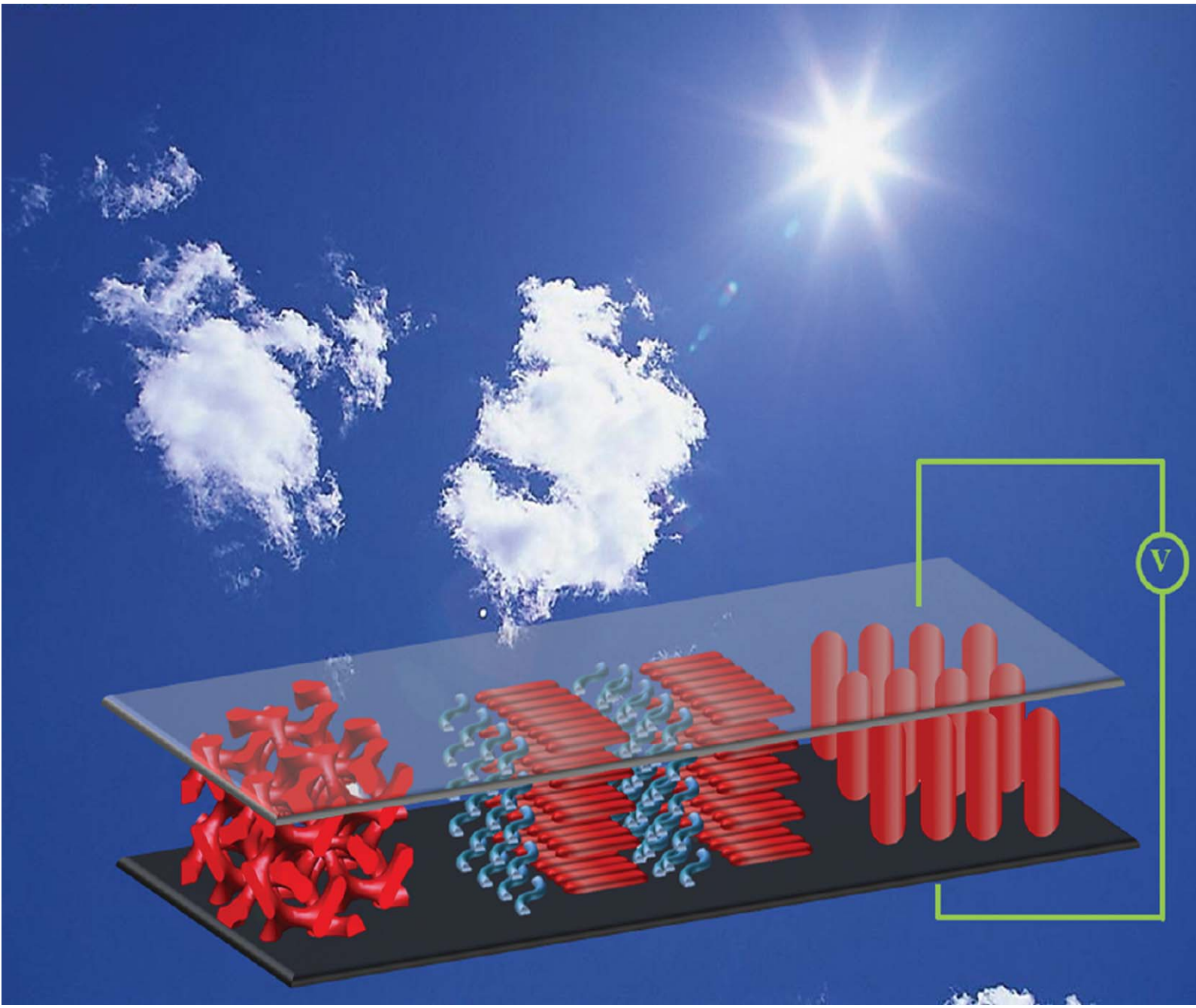

ISSN 0959-9428

RSC Publishing

FEATURE ARTICLE

Zhiqun Lin *et al.*

Conjugated rod–coil and rod–rod block copolymers for photovoltaic applications

International Year of CHEMISTRY 2011

0959-9428(2011)21:43;1-E

Journal of Materials Chemistry

Dynamic Article Links

Cite this: *J. Mater. Chem.*, 2011, **21**, 17039

www.rsc.org/materials

FEATURE ARTICLE

Conjugated rod–coil and rod–rod block copolymers for photovoltaic applications

Ming He,[ab] Feng Qiu[b] and Zhiqun Lin*[ac]

Received 10th April 2011, Accepted 20th June 2011
DOI: 10.1039/c1jm11518a

Conjugated polymer-based bulk heterojunction (BHJ) solar cells are widely recognized as a promising alternative to their inorganic counterparts for achieving low-cost, roll-to-roll production of large-area flexible lightweight photovoltaic devices. Current research in designing new polymers and optimizing device architectures has been devoted to improving the film morphology, photovoltaic performance and stability of polymer BHJ solar cells. Conjugated block copolymers (BCPs), including rod–coil and rod–rod BCPs, exhibit excellent flexibility for tuning the band gap of semiconductor polymers, regulating the molecular organization of donor (and/or acceptor) units, templating the film morphology of active layers, and achieving well-defined BHJ architectures. In this Feature Article, we summarize the recent developments over the past five years in the synthesis, self-assembly, and utilization of conjugated rod–coil and all-conjugated rod–rod BCPs for solar energy conversion, highlight the correlation between the microphase-separated morphology and photovoltaic properties in conjugated BCPs, and finally provide an outlook on the future of BCP-based photovoltaic devices.

[a]*Department of Materials Science and Engineering, Iowa State University, Ames, IA, 50011, USA. E-mail: zqlin@iastate.edu*
[b]*The Key Laboratory of Molecular Engineering of Polymers, Ministry of Education, Department of Macromolecular Science, Fudan University, Shanghai, 200433, China*
[c]*School of Materials Science and Engineering, Georgia Institute of Technology, Atlanta, GA, 30332, USA. E-mail: zhiqun.lin@mse.gatech.edu*

1. Introduction

1.1 Conjugated polymer solar cells

Conjugated polymer-based photovoltaic devices have received considerable attention as they offer exceptional potential for achieving lightweight, flexible, low-cost solar cells. During the last five years, significant advances have been made in rationally

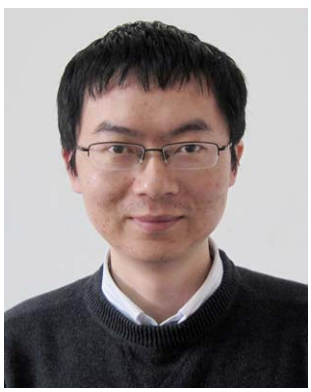

Ming He

Ming He received the PhD degree in Polymer Chemistry and Physics from Fudan University, Shanghai, China in 2011, under the supervision of Professor Feng Qiu. He worked with Professor Zhiqun Lin at Iowa State University, USA as a visiting student from October 2009 to March 2011. His graduate research mainly focuses on the synthesis, self-assembly, and utilization of conjugated polymers for photovoltaics. His research interests also include the synthesis of inorganic quantum dots, nanostructured solar cells, and thermoelectrical nanocomposites.

Feng Qiu

Feng Qiu received the Master degree in Engineering from Shanghai Institute of Metallurgy, Chinese Academy of Sciences in 1995, and the PhD degree in Polymer Chemistry and Physics from Fudan University in 1998. He was a postdoctoral research associate at University of Pittsburgh. In 2001 he joined Fudan University as an Associate Professor at the Department of Macromolecular Science, and was promoted to Professor in 2003. His research activities primarily involve the equilibrium and dynamical properties of complex block copolymers, polymer solutions, and thin films. He received China National Funds for Distinguished Young Scientists in 2006.

designing new conjugated polymers (CPs) and engineering photoactive nanostructure architectures, thereby leading to improved power conversion efficiency (PCE), which recently has exceeded 8%.[1–3] Polymer solar cells have relatively low PCE compared to inorganic solar cells, for which the maximum PCE approaches 40% for GaInP/GaInAs solar cells, 30% for Si solar cells and 20% for copper indium gallium selenide (CIGSe) solar cells.[4,5] However, the fabrication cost of polymer solar cells is much lower than their inorganic counterparts, making them an attractive low-cost alternative to inorganic solar cells, which usually suffer from a high cost of manufacturing and installation. Polymer solar cells carry many advantages peculiar to conjugated polymers.[2,6,7] Most CPs have optical absorption coefficient larger than 10^{-7} m^{-1}, and thus a CP film with a thickness of only 100–200 nm is capable of efficiently absorbing the sunlight; this is in sharp contrast to the 1 μm thick inorganic semiconductor film needed in inorganic-based solar cells. CPs with proper side chains can be readily spin-coated or roll-to-roll printed through solution-based processes, thereby facilitating device fabrication. The intrinsic flexibility of CPs renders the production of large-area soft polymer solar cells. Achieving low-cost, high-performance polymer solar cells requires optimization of photon absorption, exciton diffusion, photo-induced charge transfer at the donor/acceptor interface, and effective charge transport to the respective electrodes.[8–10]

1.2 Working principle of conjugated polymer solar cells

Due to the low dielectric constant of organic phases (typically $\varepsilon = 3$–4) and weak non-covalent electronic interactions between organic molecules, photogenerated excitons (*i.e.*, electron and hole pairs) in polymer solar cells are strongly bound by Coulombic force.[6,11,12] The band gap (E_g) between the highest occupied molecular orbital (HOMO) and the lowest unoccupied molecular orbital (LUMO) of the electron-donor molecule (Fig. 1a) is insufficient to break up the Coulombic force that binds the excitons.[13,14] Instead, the excitons need to diffuse to the donor/acceptor interface, where the interface potential field (V_b) arising from the energy offset between the HOMO of electron-donor molecule and the LUMO of electron-acceptor molecule dissociates excitons into free charge carriers (*i.e.*, electrons and holes). Subsequently, free charge carriers transport to the respective electrodes by a hopping process, driven by the electric field between electrodes.[12,15–17] Fullerene and its derivatives (*e.g.*, [6,6]-phenyl-C_{61}-butyric acid methyl ester ($PC_{61}BM$) and [6,6]-phenyl-C_{71}-butyric acid methyl ester ($PC_{71}BM$); Fig. 1b) are widely recognized as the best acceptors for polymer solar cells, due mainly to (1) high electron affinity to organic donors; (2) high electron mobility of up to 1 cm^2 V^{-1} s^{-1}; and (3) ultrafast photoinduced charge transfer in polymer/fullerene blend.[18] One of the grand challenges in developing ideal electron-donor polymers is to rationally design and synthesize CPs that simultaneously possess strong light absorption ability, high charge mobility and suitable HOMO–LUMO offset with the acceptors (*i.e.*, fullerene and its derivatives). Specifically, it is highly desirable to develop new CPs with broad light absorption *via* narrowing the E_g. One of the most straightforward ways is to simply either raise the HOMO level or lower the LUMO level of polymers.[18] However, the LUMO level of CPs must be at least 0.3 eV higher than that of acceptors when blending with fullerene and its derivatives in order to ensure the downhill driving force (E_d) for the energetically favorable electron transfer.[19–21] If the HOMO level of CPs moves upward to fulfill a reduced E_g for an enhanced light absorption, the open-circuit voltage, V_{oc}, proportional to the energy offset (V_b) between the HOMO of CPs and the LUMO of fullerenes will be reduced. Taken together, the magnitude of E_g and the position of the HOMO and LUMO levels of CPs need to be optimized.[19] Moreover, in order to effectively generate photocurrent and transfer charge in polymer solar cells, appropriate donor/acceptor interfaces and device architectures must be developed.

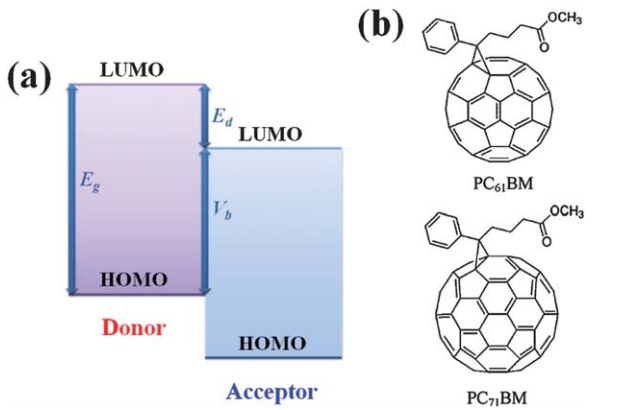

Fig. 1 (a) The HOMO and LUMO energy levels of donor and acceptor molecules, where E_g is the band gap of donor molecule, E_d is the LUMO energy offset between donor and acceptor molecules, and V_b is the interface potential field arising from the energy offset between the HOMO of donor molecules and the LUMO of acceptor molecules. (b) Chemical structures of [6,6]-phenyl-C_{61}-butyric acid methyl ester ($PC_{61}BM$) and [6,6]-phenyl-C_{71}-butyric acid methyl ester ($PC_{71}BM$). Both $PC_{61}BM$ and $PC_{71}BM$ are the most commonly used electron acceptors for polymer solar cells.

Zhiqun Lin

Zhiqun Lin received the Master degree in Macromolecular Science from Fudan University, Shanghai in 1998, and the PhD degree in Polymer Science and Engineering from UMass, Amherst in 2002. He was a postdoctoral associate at UIUC. He joined the Department of Materials Science and Engineering at Iowa State University in 2004, and was promoted to Associate Professor in 2010. He moved to Georgia Institute of Technology in 2011. His research interests include solar cells, conjugated polymers, block copolymers, polymer blends, hierarchical structure formation and assembly, surface and interfacial properties, multifunctional nanocrystals. He is a recipient of an NSF Career Award.

Three typical device architectures of polymer solar cells have been widely explored, *i.e.*, single layer, bilayer, and bulk heterojunction as schematically illustrated in Fig. 2. The single-layer architecture is the simplest device configuration, consisting of a single CP layer sandwiched between two different conducting electrodes, typically indium tin oxide (ITO) and a low work function metal such as Al, Ca or Mg (Fig. 2a).[22] The difference in work functions establishes a built-in electric field that breaks the symmetry, thereby providing a driving force for photogenerated electrons and holes toward their respective electrodes.[22,23] But the electric field arising from the difference of work functions is too weak to overcome the strong tendency for recombination between electrons and holes, resulting in low external quantum efficiency (EQE) and PCE.[24] With the donor–acceptor bilayer heterojunction confined between two conducting electrodes, the bilayer architecture offers a planar donor/acceptor interface to dissociate excitons through the interface potential field originated from the energy offset between the donor and acceptor layers (Fig. 2b).[25] This architecture also provides a direct pathway for transport of free charge carriers as the electron-donor layer is usually a *p*-type semiconductor (*i.e.*, CP) for hole transport and the electron-acceptor layer is an *n*-type semiconductor for electron transport.[26] However, a film thickness of at least 100 nm is needed for CP to efficiently absorb the incident photons, and the exciton diffusion length in most CPs is at the 10 nm length scale. As a result, only photogenerated excitons near the donor/acceptor interface at the 10 nm length scale can be dissociated into free charge carriers prior to recombination and the performance of bilayer polymer solar cells is thus greatly limited.[27–29] In this context, the bulk heterojunction (BHJ) architecture was developed to improve the PCE, in which films containing donor and acceptor semiconductors with offset energy levels interpenetrate at an approximately 10 nm length scale.[30,31]

In a typical polymer BHJ solar cell, the device performance depends heavily on the film morphology of the photoactive layer (Fig. 2c). The thoroughly mixed donor and acceptor domains introduce a large donor/acceptor interfacial area for effective exciton dissociation, where the domain is in close dimension to the exciton diffusion length (~10 nm) to allow excitons to diffuse to the donor/acceptor interface to be dissociated.[18] At the same time, each phase-separated domain should form an interpenetrated network to promote quick transport of dissociated free electrons and holes to their respective electrodes to minimize recombination, thereby resulting in high internal quantum efficiencies (IQEs), which can reach 100% in some polymer BHJ solar cells.[18,32] Considerable work has been done to control the film morphology of the photoactive layer in polymer BHJ solar cells. Self-assembly stands out as an extremely simple, inexpensive route to achieving nanoscale phase separation and forming a bicontinuous pathway for each phase.[33] Several extrinsic and intrinsic factors determine the self-assembly of CPs in the photoactive layer. The former includes all parameters associated with the device fabrication, such as the solvent used,[34,35] film thickness,[36] deposition methods,[37] film-aging time,[38] and precise control of the post-treatment procedures.[39] Most research on the improvement of film morphology focuses on the optimization of these parameters, and especially on the application of thermal annealing,[40] solvent annealing,[41] and additive.[42] The intrinsic factors are related to the interactions between the donor and acceptor molecules, relying mostly on the molecular weight,[43] the ratio of donor to acceptor,[44] crystallization, and miscibility.[45,46]

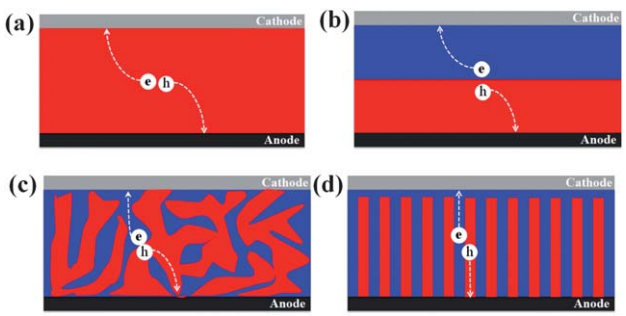

Fig. 2 Different device architectures of polymer solar cells. (a) Single layer device; (b) bilayer device; (c) bulk heterojunction device; and (d) ordered bulk heterojunction device. The red and blue domains correspond to electron donor and electron acceptor phase, respectively.

1.3 Conjugated block copolymer solar cells

Block copolymers (BCPs) consisting of two or more chemically distinct chains covalently linked at one end are thermodynamically driven to self-assemble into well-ordered nanostructured morphologies, including lamellae, cylinders, and interconnected networks, depending on the relative volume fraction of the components. In addition, the domain size is dictated by the molecular weight of copolymer and can be readily tailored to coincide with the exciton diffusion length, thereby providing a potentially optimized morphology for charge generation and transport for use in polymer solar cells.[47–50] One commonly proposed ideal morphology is depicted in Fig. 2d. Notably, most studies on the microphase separation of BCPs have focused on coil–coil BCPs with flexible polymer chain in each block. The formation of ordered nanoscopic domains depends strongly on the minimization of free energy composed of the segment-segment interaction (*i.e.*, enthalpy) and the stretching of polymer chains (*i.e.*, entropy).[51] Various thermodynamically equilibrium morphologies of coil–coil BCPs can be tuned by adjusting the volume fraction of each block ϕ, the Flory–Huggins interaction parameter χ (reflecting the degree of incompatibility between two blocks), and the degree of polymerization N, as shown in Fig. 3.[47,52–58] It is worth noting that many technologically relevant morphologies may be achieved when BCPs are confined in a thin film, enabling them to be utilized for patterning and templating the photoactive layers in organic photovoltaics.[59–61]

BCPs directly used as photovoltaic active layers usually carry at least one semiconductor block, *i.e.*, conjugated polymer. The conjugated block in BCPs is often described as the rod-like block because it is rigid compared to the flexible coil block. In so-called rod–coil BCPs, the rigid rod-like block complicates the phase behavior of BCPs. The liquid crystalline interaction and the topological disparity between the rod and coil blocks require the introduction of two additional parameters. One is the Maier–Saupe interaction strength, μN, characterizing the aligning interaction between the rod blocks, and the other is the geometrical asymmetry, ν, defined as the ratio between the coil

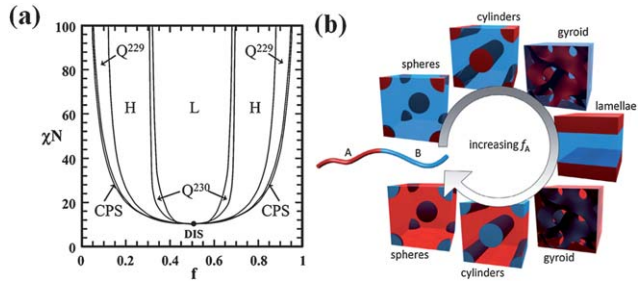

Fig. 3 (a) Theoretical phase diagram of a typical coil–coil block copolymers, where L, H, Q^{229}, Q^{230}, CPS, and DIS correspond to the lamellae, hexagonally packed cylinder, body-centered sphere, double-gyroid, closed-packed sphere, and disordered phases, respectively. Adapted with permission from ref. 56. Copyright © 2006 American Chemical Society. (b) Schematic illustration of various phases in (a). Adapted with permission from ref. 57. Copyright © 2010 Elsevier Ltd.

radius of gyration and the rod length.[33,62,63] Thus in rod–coil BCPs, the equilibrium phase separation is governed by four parameters, that is, the chain stretching, the Flory–Huggins interaction parameter χ, the Maier–Saupe interaction, and the geometrical asymmetry, leading to completely different nanostructures (Fig. 4) from those of coil–coil BCPs and resulting in varied photovoltaic performances.[64] Compared to widely studied coil–coil BCPs, due primarily to the rigid nature of rod-like blocks that complicates the synthesis and self-assembly, far less attention has been focused on the understanding of synthetic methods, self-assembly mechanism, and physical properties of conjugated BCPs. Recent advances in synthetic techniques render the rational design and synthesis of target rod-like blocks and offer expanded flexibility for realizing high-performance conjugated BCPs.

This Feature Article seeks to summarize the recent developments over the past five years in the synthesis, self-assembly, and utilization of conjugated rod–coil and all-conjugated rod–rod BCP for solar energy conversion, highlight the correlation between the microphase-separated morphology and photovoltaic properties in conjugated BCPs, and finally provide an outlook on the future of BCP-based photovoltaic devices.

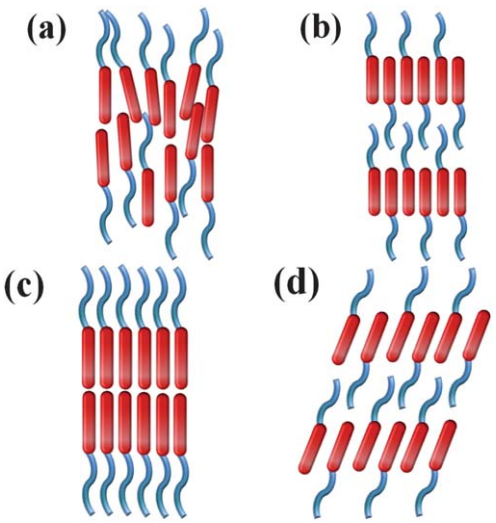

Fig. 4 Schematic of rod–coil block copolymers self-assembled into (a) nematic phase, (b) monolayer smectic A phase, (c) bilayer smectic A phase, and (d) monolayer smectic C phase.

2. Rod–coil block copolymers

The donor–acceptor blend in polymer BHJ solar cells exhibits significant structural disorder due to uncontrollable phase separation. Despite the fact that the processing conditions can be tuned, including the choice of casting solvent, solvent evaporation rate, and thermal or solvent annealing, it remains challenging to fully control the domain size and eliminate the formation of dead ends in the blend, which lead to large excitonic loss and charge recombination.[63] The motivation to develop rod–coil BCPs for photovoltaic applications lies in the incorporation of a functional semiconductor block into the equilibrium ordered nanostructures. The extension of the π orbital along the semiconductor polymers renders them with unique optical and electronic properties, and meanwhile makes the polymer backbone rigid to yield a rod-like configuration, thus introducing additional geometrical constraints for phase separation.[65] A proper choice of flexible coil block linked to rigid conjugated rod-like block would mitigate such geometrical constrains, thereby facilitating the nanoscale phase separation.[66,67] In contrast to simple blending, chemically bonded rod–coil blocks are constrained by microphase separation into distinct domains, the widths of which are close to the length of polymer chains. The microphase separation of rod–coil BCPs provides the possibility to create highly ordered heterojunction structures for efficient charge generation, where the domain size is controllable by the length of blocks (*i.e.*, molecular weight) and, at the same time, form bicontinuous network in each phase for effective charge transfer.[68–70]

2.1 Phase behaviors of rod–coil block copolymers

In order to explore the phase behavior and self-assembly mechanism of rod–coil BCPs, synthesis of a BCP with well-defined nanostructures is required. Two typical synthetic strategies for preparing rod–coil BCPs have been developed, which are well suited to incorporate coil components into conjugated rod-like blocks. In the 'grafting-from' approach, the rod-like macroinitiator is firstly prepared and used to initiate the living polymerization of coil block.[71,72] In the 'grafting-to' approach, rod and coil blocks with complimentary functional groups are independently synthesized and subsequently tethered together by a coupling reaction (*e.g.*, macrotermination, acid–base chemistry,[73] or "click" chemistry[74,75]). The competition between the Flory–Huggins interaction and Maier–Saupe interaction plays a crucial role in the self-assembly of rod–coil BCPs.[33]

Because of its high crystallinity, good electrical conductivity, and photoluminescent properties, poly(*p*-phenylenevinylene) (PPV) has attracted a great deal of attention.[76,77] PPV and its derivatives remain one of the most widely studied CPs for use in optoelectronics.[78–80] Due to strong π-conjugated interactions between the aromatic backbones, PPV can hardly dissolve in organic solvents. A general methodology to circumvent this problem is to incorporate alkyl side chain into the PPV backbone or integrate soluble blocks to one end of PPV chain, which also alters the electronic and optical properties of PPV.[69,73,81–83]

Alternatively, PPV-based rod–coil BCPs can also be prepared in which a rigid PPV block serves as an electron-donor and a flexible coil block is chosen to allow for the solubility of BCPs in organic solvents, leading to varied phase-separated morphologies. For weakly segregated BCPs, such as poly(diethylhexyloxy)-*p*-phenylenevinylene)-*b*-polyisoprene (DEH–PPV-*b*-PI) (Fig. 5a), order–disorder and nematic–isotropic transitions can be accessed because of the thermodynamic compatibility of PPV rods and PI coils. At high temperature and high volume fraction of PI coils, DEH–PPV-*b*-PI exhibited an isotropic phase with the transition to a broad nematic region followed by lamellar phases as the temperature decreased. Furthermore, at some volume fractions, there was a change in domain spacing, suggesting a reorientation of rods within the lamellae.[66] The phase diagram derived from the experimental observations was in qualitative agreement with the theoretical phase diagram of weak segregation limit BCPs, showing phase transitions between lamellar, nematic and isotropic phases.[84,85] For intermediately segregated BCPs, such as poly(diethylhexyloxy)-*p*-phenylenevinylene)-*b*-poly(methyl methacrylate) (DEH–PPV-*b*-PMMA) (Fig. 5b), the copolymer self-assembled into smectic-lamellar structures at low coil fraction and into smectic-hexagonal structures at higher coil fraction (Fig. 5c), and the segregation between the rods and coils was strong enough to allow the rods to be unaffected by the presence of a microdomain boundary.[73] For strongly segregated BCPs,[86] their phase behavior is close to that of rod–rod BCPs, which is largely dominated by the competition between phase separation and crystallization of distinct rigid blocks.

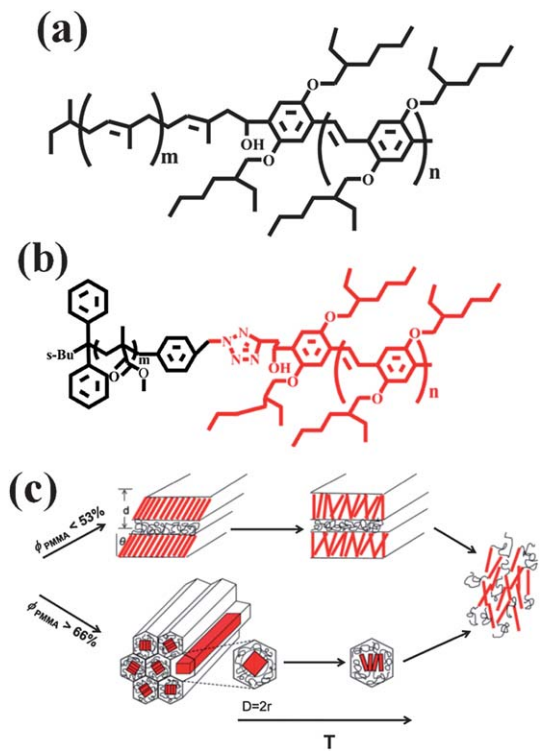

Fig. 5 (a) Chemical structure of DEH–PPV-*b*-PI. (b) Chemical structure of DEH–PPV-*b*-PMMA. (c) Schematic illustration of possible rod segment packing in rod–coil PPV-*b*-PMMA block copolymers; the lamellar and hexagonal structures are shown on the top and bottom panels, respectively. When the volume fraction of coil-like PMMA block (black) is lower than 53%, the rigid rod-like DEH–PPV blocks aggregate into lamellae. At higher coil volume fraction, the rods are organized into hexagons. Adapted with permission from ref. 73. Copyright © 2009 American Chemical Society.

2.2 Photovoltaic performance of rod–coil block copolymers

By grafting an electron-acceptor group onto the coil block in rod–coil BCPs, the resulting rod–coil BCP possesses both the semiconductor donor and acceptor.[35,82,87] One typical donor–acceptor rod–coil BCP is based on DEH–PPV coupled with a fullerene-substituted polystyrene (PS). Modified DEH–PPV was used as macroinitiator in the controlled atom transfer radical polymerization (ATRP) to yield DEH–PPV-*b*-PS with chloromethyl group on the PS block, followed by the addition of fullerene to chloromethyl group through ATRP. A strong photoluminescence quenching was observed, suggesting the presence of large donor/acceptor interface between PPV-aligned crystalline domains and grafted fullerene molecules.[70,88,89] However, the incorporation of fullerene into the coil block in rod–coil BCPs considerably influenced the self-assembly of BCPs due to the growth of fullerene nanocrystals that hindered the formation of an ordered phase (*e.g.*, lamella and cylinder), and the resulting thin film nanostructures may not be optimized for high PCE devices.[70] To this end, donor-bridge–acceptor type BCPs were developed, where the addition of a flexible, large band-gap bridge block not only retarded electron–hole recombination between the donor and acceptor blocks, but also promoted the rigid donor and acceptor segments to self-assemble into potential lamellar structures for effective charge transfer. The introduction of a bridge block significantly improved V_{oc}, but the photocurrent was still very low, due primarily to the insulating characteristic of the bridge block.[50,90–92]

With recent advances made in Grignard metathesis (GRIM) polymerization of poly(3-alkylthiophene) (P3ATs),[93] P3AT-based photovoltaic devices—in particular, poly(3-hexylthiophene) (P3HT)—have become the focus of research. The quasi-living reaction of the GRIM method makes it possible and easy to introduce a coil block possessing complementary functional groups that can react with end-functionalized P3HT, thereby providing more opportunities to tailor the self-assembly and photovoltaic properties of P3AT-based rod–coil BCPs.[94,95] One of the most intensively studied P3AT-based photovoltaics is the P3HT:PCBM BHJ solar cell, in which a reproducible 3–5% PCE has been achieved by optimizing the molecular organization of P3HT and the film morphology of the P3HT/PCBM blend.[96–101] The design and synthesis of well-defined 'donor–acceptor rod–coil' BCPs consisting of donor P3HT and acceptor PCBM are expected to yield more preferable nanostructures (*e.g.*, lamellae or cylinder) than the P3HT/PCBM randomly mixed blend.[102] Multi-step synthesis based on GRIM polymerization and living polymerization has been demonstrated as a promising route to P3HT-*b*-fullerene-based rod–coil BCPs. A typical synthesis of P3HT-*b*-fullerene BCP included the following three steps (Scheme 1):[103] (1) an end-functionalized regioregular P3HT was synthesized through GRIM polymerization; (2) methyl methacrylate (MMA) and 2-hydroxyethyl methacrylate (HEMA) were copolymerized by using the end-functionalized P3HT as macroinitiator for ATRP to yield P3HT-*b*-P(MMA-*r*-

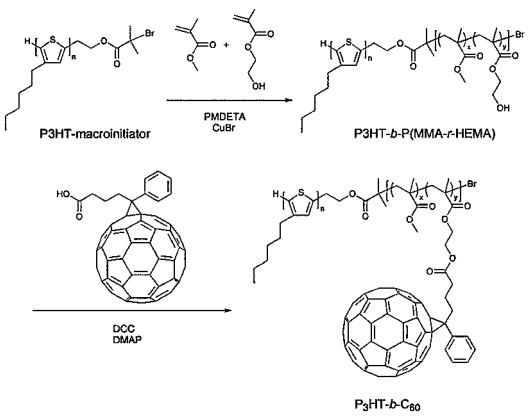

Scheme 1 Synthesis of P3HT-*b*-fullerene block copolymers, where PMDETA is *N*,*N*,*N*′,*N*′,*N*″-pentamethyldiethylenetriamine, DCC is 1,3-dicylohexylcarbodiimide, DMAP is dimethylaminopyridine, and C_{60} is fullerene. Adapted with permission from ref. 103. Copyright © 2009 Royal Society of Chemistry.

HEMA) BCP; and (3) fullerene functionalized with carboxylic acid, [6,6]-phenyl-C_{61}-butyric acid (PCBA), was then chemically linked to the HEMA unit in P(MMA-*r*-HEMA) to produce P3HT-*b*-fullerene BCPs. The thermally stable phase morphology of BCP was reflected in the significantly improved high-temperature stability of the performance of the resulting device that was prepared by adding a few P3HT-*b*-fullerene to the P3HT/PCBM blend, and it can be rationalized as follows: (1) the addition of P3HT-*b*-fullerene may lower the interfacial tension between P3HT and fullerene phases, leading to reduction of the size of the P3HT/PCBM blend with uniform size distribution (Fig. 6); (2) the kinetic effect by which the BCP can reduce the agglomeration rate of domains, resulting in improvement of long-term stability of device performance.[104] The use of P3HT-*b*-fullerene rod–coil BCP to control the interface morphology of P3HT/PCBM BHJ was also demonstrated in P3HT-*b*-polystyrene-polyacrylate with fullerene grafted onto the polyacrylate block (*i.e.*, P3HT-*b*-P(S_xA_y)-fullerene), which was synthesized by a combination of GRIM polymerization, reversible addition-fragmentation chain transfer (RAFT) polymerization, and polymer-analogous cycloaddition reaction.[105] By adding a small amount of P3HT-*b*-P(S_xA_y)-fullerene to the P3HT/PCBM blend, the interfacial morphology between these two immiscible components was altered, resulting in a noticeable difference in phase segregation of the BHJ film. A significantly enhanced short circuit current J_{sc} was obtained upon the addition of 5% P3HT-*b*-PSA-fullerene, leading to an approximately 35% increase in PCE to 3.5%.

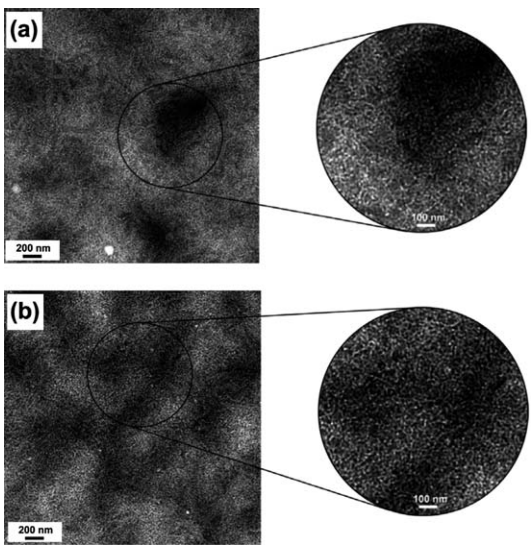

Fig. 6 TEM images of (a) a standard P3HT/PCBM film and (b) a P3HT/P3HT-*b*-fullerene/PCBM blend film with 2.5 wt% addition of P3HT-*b*-fullerene block copolymer after thermal annealing at 150 °C for 6 h. The insets show higher magnification images. In the standard P3HT/PCBH film, large aggregations of PCBM appeared as dark islands were formed. While the P3HT/PCBM blend with the addition of P3HT-*b*-fullerene exhibited weaker phase contrast, the PCBM rich phase contains a considerable number of P3HT fibrillar crystals and *vice versa*. Adapted with permission from ref. 104. Copyright © 2010 IOP Publishing Ltd.

2.3 Utilization of rod–coil block copolymer templates

Rather than being utilized as photoactive materials for photovoltaics, rod–coil BCPs can also be exploited as structure directors (*i.e.*, template).[106] Recently, P3HT-*b*-Poly(L-lactide) (P3HT-*b*-PLLA) was synthesized and employed as both an electron-donor and a structure-directing agent to pattern donor–acceptor components into ordered nanostructures as depicted in Fig. 7.[107] The characteristic period of P3HT-*b*-PLLA was

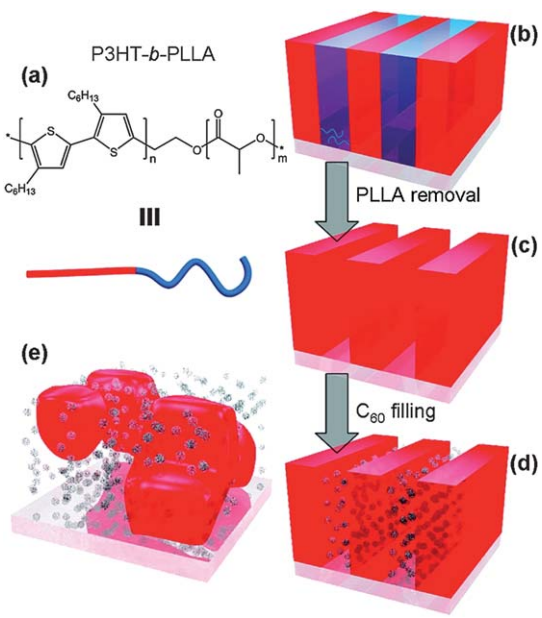

Fig. 7 (a) Chemical structure of P3HT-*b*-PLLA block copolymer and its schematic representation. (b) Ordered nanoscale thin film morphology consisting of lamellae of P3HT-*b*-PLLA oriented perpendicular to the substrate. (c) Ordered P3HT donor lamellae after the removal of biodegradable PLLA block. (d and e) Comparison of an ordered nanoscale morphology consisting of self-assembled P3HT donor lamellae that were separated by C_{60} acceptor in (d), and a less ordered morphology obtained when simply blending P3HT donor homopolymer with C_{60} acceptors in (e). Adapted with permission from ref. 107. Copyright © 2009 American Chemical Society.

designed to be about 15 nm, comparable to the 10 nm exciton diffusion length. The additional advantage of using P3HT-*b*-PLLA was that the coil-like PLLA block is biodegradable. Thus, upon the formation of ordered nanoscale morphology due to the microphase separation of two incompatible P3HT and PLLA blocks, the PLLA block can be readily removed and replenished with fullerene derivatives or other acceptor molecules (Fig. 7d).[108] As such, a new ordered donor–acceptor morphology consisting of alternating donor–acceptor nanostructured domains was formed and is expected to enhance the effectiveness of internal processes (*i.e.*, charge generation at the donor/acceptor interface and charge transport in the blend film) as compared to a less ordered BHJ morphology obtained by simply mixing donor and acceptor molecules (Fig. 7e).

3. Rod–rod block copolymers

Although the coil block facilitates controlled and thermally stable microphase separation, its insulating characteristic limits the use of rod–coil BCPs in electronic and photovoltaic devices. In this regard, recently all-conjugated rod–rod BCPs have received much attention because of their attractive combination of self-assembly and electronic activity.[109–112] The key to developing rod–rod BCPs lies in not only tailoring their self-assembly behavior, but also rendering two blocks with the electron donor on one block and the electron acceptor on the other block, forming BCPs that can be engineered to perform semiconductor p–n junctions with well-defined nanostructures.[113] Owing to the high persistence length of the individual conjugated block and the extended π-electrons along the neighboring conjugated block (*i.e.*, intrachain),[114,115] all-conjugated BCPs allow for an organization of the copolymer chains into large-area ordered lamellar nanostructures, the size of which is commensurate with the exciton diffusion length.[116] The synthesis and self-assembly of rod–rod BCPs that combine both intriguing nanostructures and electronic activity provide expanded opportunities for developing high-performance polymer BHJ solar cells. However, the rigid rod-like polymer chains make the conventional methods used for synthesis of coil–coil and rod–coil BCPs, especially living anionic polymerization, most often not applicable for rod–rod BCPs.[64] With the development of extremely effective and controllable GRIM polymerization of P3ATs, which was then extended to synthesis of polyphenylenes, polyfluorenes and polypyrroles,[117–119] the GRIM chain-growth polycondensation has become the most attractive method for synthesis of CPs and all-conjugated rod–rod BCPs.[109,119,120]

3.1 Rod–rod block copolymers as donor materials

Polymer BHJ solar cells based on all-conjugated poly(3-butylthiophene)-*b*-poly(3-octylthiophene) (P3BT-*b*-P3OT) exhibited PCE as high as 3.0% when blended with $PC_{71}BM$, which was much higher than the corresponding homopolymer-based devices.[121] The idea behind the molecular design of all-conjugated P3BT-*b*-P3OT BCPs was to incorporate different alkyl side chains into the rod–rod BCPs to balance and optimize the solubility, self-assembly, and π-stacking effects of the insulating side groups, and thus the electronic and optoelectronic properties. AFM and TEM imaging in conjunction with XRD results showed that the P3BT-*b*-P3OT/$PC_{71}BM$ blend had an interpenetrating morphology with the size of crystalline polymer domains of 11–18 nm. The largely improved photovoltaic efficiency was due to the enhanced carrier mobility of holes in the BHJ devices, where the P3BT block with short butyl side led to the enhanced self-assembly of polymer chains. Recently, all-conjugated poly(3-butylthiophene)-*b*-poly(3-hexylthiophene) (P3BT-*b*-P3HT) BCPs were demonstrated to experience different kinetic pathways from the P3BT and P3HT homopolymers when they self-assembled in the mixed solvents of anisole/chloroform.[122] The change in the anisole/chloroform ratio exerted a profound influence on the assembly of P3BT-*b*-P3HT chains, leading to the formation of varied nanostructured morphologies. Uniformly dispersed, high-aspect-ratio P3BT-*b*-P3HT nanowires with a diameter of 8–10 nm and a length of micrometers were readily achieved in the anisole/chloroform $\leq 2:1$ solutions. Quite intriguingly, by increasing anisole (*i.e.*, anisole/chloroform $\geq 6:1$), P3BT-*b*-P3HT chains self-assembled into two-dimensional nanorings, which were promoted by the enhanced solvophobic interaction between P3BT-*b*-P3HT blocks and anisole,[123] thereby minimizing the unfavorable interfacial area per unit volume in the solution.[124]

Compared to P3AT homopolymer counterparts, better optimized polymer BHJ nanostructures were then achieved in P3BT-*b*-P3HT/$PC_{71}BM$ solar cells by tuning the ratio of two dissimilar blocks of P3BT and P3HT in the BCPs (Fig. 8).[125,126] An attractive PCE of 4.02% was yielded, which was a direct consequence of the formation of small crystalline domains of 10.4 nm

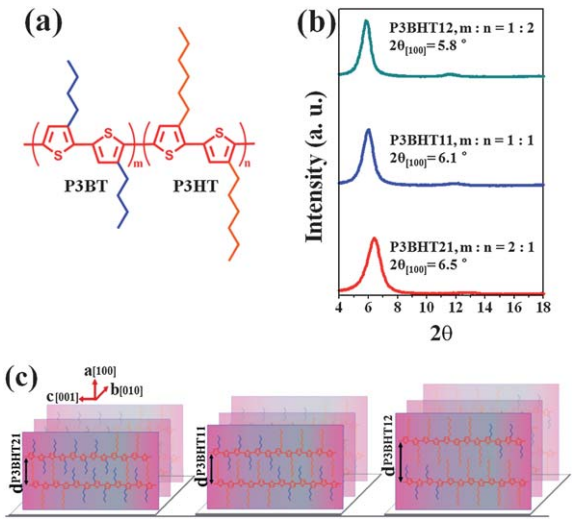

Fig. 8 (a) Chemical structure of poly(3-butylthiophene)-*b*-poly(3-hexylthiophene) (P3BHT) diblock copolymer. (b) XRD profiles of P3BHT films prepared from the P3BHT *o*-dichlorobenzene solution. The diblock copolymers with different lengths of alkyl side chain used in the study were P3BHT21 (P3BT:P3HT = 2 : 1, mol/mol), P3BHT11 (P3BT:P3HT = 1 : 1, mol/mol), and P3BHT12 (P3BT:P3HT = 1 : 2, mol/mol). (c) Schematic representation of P3BHT21 (left panel), P3BHT11 (central panel), and P3BHT12 (right panel) lamella packing with the edge-on orientation. P3BHT diblock copolymers with different alkyl chain lengths tend to co-crystallize forming a crystalline lamellar by interdigitating two different side chains, each with tunable interchain distance along the (100) axis (*i.e.*, side-chain direction).

that is comparable to the exciton diffusion length in P3ATs, finer phase separation on the nanoscale with a homogeneous donor–acceptor interface to maximize the charge generation, and percolation networks with hole mobility of 2.0×10^{-4} cm^2 V^{-1} s^{-1} for the charge transport and collection. The strategy of precisely controlling the ratio of the blocks in all-conjugated block copolymer to yield improved photovoltaic performance may provide insight into many aspects of solar energy conversion, from rational design and synthesis of new materials to engineering of high-efficiency polymer BHJ solar cells.

3.2 Rod–rod block copolymer as donor–acceptor materials

Compared to the donor–acceptor rod–coil BCPs, the use of donor–acceptor all-conjugated rod–rod BCPs is advantageous as the charge carrier mobility is increased.[50] In donor–acceptor all-conjugated rod–rod BCP, one rod block acts as electron-donor while the other functions as electron-acceptor. Perylene diimide and its derivatives are known as good electron-acceptor materials with high electron mobility of up to 2.1 cm^2 V^{-1} s^{-1}.[127–129] Several methods based on a combination of GRIM polymerization and living radical polymerization have been exploited to synthesize poly(3-hexylthiophene)-*b*-poly(perylene diimide acrylate) (P3HT-*b*-PPDA) donor–acceptor all-conjugated BCPs. Remarkable differences in PCEs were observed in P3HT-*b*-PPDA synthesized and fabricated into solar cells under different processes. The P3HT-*b*-PPDA synthesized by combining GRIM polymerization and click reaction showed PCEs up to 0.03%.[130] In a different synthetic approach involving GRIM polymerization and subsequent nitroxide mediated radical polymerization (NMRP), vinyl-terminated P3HT was synthesized by GRIM polymerization and converted to alkoxyamine macroinitiator, which was then used in the controlled NMRP of PDA.[131] Integrating P3HT and the perylene units into a BCP structure limited the nanoscale phase separation between the donor and acceptor blocks, which was responsible for a higher PCE of 0.49% in P3HT-*b*-PPDA BCPs than that of 0.18% in donor/acceptor blends.[132] The molecular weight of P3HT-*b*-PPDA was also found to influence the photovoltaic performance. The devices made from P3HT-*b*-PPDA with higher molecular weight ($M_{n,P3HT}$ = 17 kg mol^{-1}, PPDA = 55 wt%) exhibited 20-fold improvement in PCEs compared to that of lower molecular weight used ($M_{n,P3HT}$ = 9 kg mol^{-1}, PPDA = 55 wt%).[133] One of the best working examples of all-conjugated donor–acceptor BCPs is a fullerene-attached all-conjugated polythiophene BCP with a well-defined structure, which has an advantage of controlling the film morphology and improving the morphological stability of the film, resulting in a PCE near 2%.[134]

4. Conclusions and outlook

Rapid advances have been witnessed in improving photovoltaic performance of polymer solar cells over the past five years. Current research efforts are directed toward elucidating photophysical phenomena (*i.e.*, exciton generation, diffusion and dissociation as well as charge transport and collection) and mechanisms responsible for the enhanced performance. The ideal semiconductor polymers for use as promising photovoltaic materials should fulfill several requirements: (1) a band gap (E_g) between 1.30 and 1.90 eV to expand the spectral absorption domain and more efficiently harvest the photon flux spectrum of sunlight; (2) a well-matched energy offset between the HOMO of donor and the LUMO of acceptor to maximize V_{oc}; (3) a high donor–acceptor interfacial area to facilitate exciton dissociation; (4) a bicontinuous network with domain width twice the exciton diffusion length to optimize the charge generation and transport.[2,18] Compared to homopolymers, BCPs are of particular interest for photovoltaic applications because of their superior self-assembly characteristic and improved control over nanoscale morphology. Recent development in synthesis techniques, in particular, GRIM polymerization, have rendered rational molecular design and synthesis of a wide variety of rod–coil and rod–rod BCPs, opening numerous opportunities for producing nanostructured functional BCP-based BHJ solar cells.

Future development of BCP-based solar cells will center on simultaneous optimization of the photophysical structure (*i.e.*, the HOMO–LUMO level of BCP), molecular organization, and film morphology to achieve high-performance photovoltaic devices. To this end, the first approach is to craft ordered polymer BHJ nanostructures through fine tuning the chemical composition of each block, the block length (*i.e.*, molecular weight), and the block ratio. The ability to control the Flory–Huggins interaction, the Maier–Saupe interaction and the geometrical asymmetry in rod–coil BCPs would afford a potentially viable route to ideal nanostructures for solar energy conversion. One may even extend the use of rod–coil or rod–rod BCPs in which one block can be selectively removed to yield the structure director for assembling ordered donor/acceptor interface. A pioneering work has been demonstrated by capitalizing on P3HT-*b*-PLLA BCPs,[107] where the PLLA block was easily degraded, leaving behind regular layered P3HT nanodomains. Subsequently, the inter-space between adjacent domains was impregnated with fullerenes to attain well-defined P3HT-fullerene layered nanostructures, thereby meeting all requirements of the formation of a bicontinuous network, small domain size and large donor/acceptor interface for high-efficiency solar cells. The second approach is the incorporation of electronically active molecules (*e.g.*, CPs and fullerenes) into rod or coil blocks to obtain functionalized donor–acceptor rod–coil or rod–rod BCPs, which therefore provide the expanded possibility to confine electronically active groups in geometrically well-defined nanostructures, promoting charge generation and transport.[50] A variation of electronic properties by altering the block length and type of electronic group is also feasible in rod–coil and rod–rod BCPs.[135] The third approach is to lower the band gap of CPs by combining two co-monomers, one being an electron-rich (*i.e.*, fluorine, carbazole, dibenzosilole, benzodithiophene) and the other being an electron-deficient moiety (*i.e.*, benzodiathiazole, diketopyrrolopyrrole).[136] Recently, a wide range of such push–pull alternating copolymers have been synthesized with band gaps ranging from 1.0 to 1.9 eV, HOMO energy levels lower than −5.20 ev, and PCEs exceeding over 7%. The push–pull copolymers also possess all-conjugated molecular structures. Their phase behavior and self-assembly depend largely on the choice of conjugated backbones and soluble side chains.[9] An extensive study on the relationship between molecular packing, crystallinity, film morphology and influence on charge generation and transfer in push–pull copolymers is emerging as a bright,

promising direction for designing new polymer solar cells with PCE approaching 10%.

Acknowledgements

We gratefully acknowledge the support from the National Science Foundation (NSF-CBET 0824361).

Notes and references

1 H. Y. Chen, J. H. Hou, S. Q. Zhang, Y. Y. Liang, G. W. Yang, Y. Yang, L. P. Yu, Y. Wu and G. Li, *Nat. Photonics*, 2009, **3**, 649.
2 Y. Y. Liang and L. P. Yu, *Acc. Chem. Res.*, 2010, **43**, 1227.
3 Solarmer Energy Inc., www.solarmer.com.
4 R. R. King, D. C. Law, K. M. Edmondson, C. M. Fetzer, G. S. Kinsey, H. Yoon, R. A. Sherif and N. H. Karam, *Appl. Phys. Lett.*, 2007, **90**, 183516.
5 A. Hagfeldt, G. Boschloo, L. C. Sun, L. Kloo and H. Pettersson, *Chem. Rev.*, 2010, **110**, 6595.
6 C. Deibel and V. Dyakonov, *Rep. Prog. Phys.*, 2010, **73**, 096401.
7 H. B. Wu, L. Ying, W. Yang and Y. Cao, *Chem. Soc. Rev.*, 2009, **38**, 3391.
8 B. H. Hamadani, S. Y. Jung, P. M. Haney, L. J. Richter and N. B. Zhitenev, *Nano Lett.*, 2010, **10**, 1611.
9 C. Piliego, T. W. Holcombe, J. D. Douglas, C. H. Woo, P. M. Beaujuge and J. M. J. Frechet, *J. Am. Chem. Soc.*, 2010, **132**, 7595.
10 D. Chen, A. Nakahara, D. Wei, D. Nordlund and T. P. Russell, *Nano Lett.*, 2011, **11**, 561.
11 R. Kersting, U. Lemmer, M. Deussen, H. J. Bakker, R. F. Mahrt, H. Kurz, V. I. Arkhipov, H. Bassler and E. O. Gobel, *Phys. Rev. Lett.*, 1994, **73**, 1440.
12 B. A. Gregg, *MRS Bull.*, 2005, **30**, 20.
13 E. Collini and G. D. Scholes, *Science*, 2009, **323**, 369.
14 J. L. Bredas, J. Cornil and A. J. Heeger, *Adv. Mater.*, 1996, **8**, 447.
15 T. Stubinger and W. Brutting, *J. Appl. Phys.*, 2001, **90**, 3632.
16 M. Knupfer, *Appl. Phys. A: Mater. Sci. Process.*, 2003, **77**, 623.
17 B. A. Gregg, *J. Phys. Chem. B*, 2003, **107**, 4688.
18 B. C. Thompson and J. M. J. Frechet, *Angew. Chem., Int. Ed.*, 2008, **47**, 58.
19 Y. J. Cheng, S. H. Yang and C. S. Hsu, *Chem. Rev.*, 2009, **109**, 5868.
20 L. J. A. Koster, V. D. Mihailetchi and P. W. M. Blom, *Appl. Phys. Lett.*, 2006, **88**, 093511.
21 C. J. Brabec, C. Winder, N. S. Sariciftci, J. C. Hummelen, A. Dhanabalan, P. A. van Hal and R. A. J. Janssen, *Adv. Funct. Mater.*, 2002, **12**, 709.
22 J. Nelson, *Curr. Opin. Solid State Mater. Sci.*, 2002, **6**, 87.
23 C. W. Tang, *Appl. Phys. Lett.*, 1986, **48**, 183.
24 D. Wohrle and D. Meissner, *Adv. Mater.*, 1991, **3**, 129.
25 N. S. Sariciftci, D. Braun, C. Zhang, V. I. Srdanov, A. J. Heeger, G. Stucky and F. Wudl, *Appl. Phys. Lett.*, 1993, **62**, 585.
26 A. C. Arango, L. R. Johnson, V. N. Bliznyuk, Z. Schlesinger, S. A. Carter and H. H. Horhold, *Adv. Mater.*, 2000, **12**, 1689.
27 J. J. M. Halls, K. Pichler, R. H. Friend, S. C. Moratti and A. B. Holmes, *Appl. Phys. Lett.*, 1996, **68**, 3120.
28 M. Theander, A. Yartsev, D. Zigmantas, V. Sundstrom, W. Mammo, M. R. Andersson and O. Inganas, *Phys. Rev. B: Condens. Matter*, 2000, **61**, 12957.
29 A. Haugeneder, M. Neges, C. Kallinger, W. Spirkl, U. Lemmer, J. Feldmann, U. Scherf, E. Harth, A. Gugel and K. Mullen, *Phys. Rev. B: Condens. Matter*, 1999, **59**, 15346.
30 G. Yu and A. J. Heeger, *J. Appl. Phys.*, 1995, **78**, 4510.
31 J. J. M. Halls, C. A. Walsh, N. C. Greenham, E. A. Marseglia, R. H. Friend, S. C. Moratti and A. B. Holmes, *Nature*, 1995, **376**, 498.
32 S. H. Park, A. Roy, S. Beaupre, S. Cho, N. Coates, J. S. Moon, D. Moses, M. Leclerc, K. Lee and A. J. Heeger, *Nat. Photonics*, 2009, **3**, 297.
33 R. A. Segalman, B. McCulloch, S. Kirmayer and J. J. Urban, *Macromolecules*, 2009, **42**, 9205.
34 S. E. Shaheen, C. J. Brabec, N. S. Sariciftci, F. Padinger, T. Fromherz and J. C. Hummelen, *Appl. Phys. Lett.*, 2001, **78**, 841.
35 H. Hoppe, M. Niggemann, C. Winder, J. Kraut, R. Hiesgen, A. Hinsch, D. Meissner and N. S. Sariciftci, *Adv. Funct. Mater.*, 2004, **14**, 1005.
36 H. Benten, M. Ogawa, H. Ohkita and S. Ito, *Adv. Funct. Mater.*, 2008, **18**, 1563.
37 P. T. Hammond, *Adv. Mater.*, 2004, **16**, 1271.
38 H. Xin, O. G. Reid, G. Q. Ren, F. S. Kim, D. S. Ginger and S. A. Jenekhe, *ACS Nano*, 2010, **4**, 1861.
39 H. W. Tang, G. H. Lu, L. G. Li, J. Li, Y. Z. Wang and X. N. Yang, *J. Mater. Chem.*, 2010, **20**, 683.
40 E. Verploegen, R. Mondal, C. J. Bettinger, S. Sok, M. F. Toney and Z. A. Bao, *Adv. Funct. Mater.*, 2010, **20**, 3519.
41 G. Li, Y. Yao, H. Yang, V. Shrotriya, G. Yang and Y. Yang, *Adv. Funct. Mater.*, 2007, **17**, 1636.
42 D. Di Nuzzo, A. Aguirre, M. Shahid, V. S. Gevaerts, S. C. J. Meskers and R. A. J. Janssen, *Adv. Mater.*, 2010, **22**, 4321.
43 R. C. Coffin, J. Peet, J. Rogers and G. C. Bazan, *Nat. Chem.*, 2009, **1**, 657.
44 E. G. Wang, L. T. Hou, Z. Q. Wang, S. Hellstrom, F. L. Zhang, O. Inganas and M. R. Andersson, *Adv. Mater.*, 2010, **22**, 5240.
45 Y. Y. Liang, D. Q. Feng, Y. Wu, S. T. Tsai, G. Li, C. Ray and L. P. Yu, *J. Am. Chem. Soc.*, 2009, **131**, 7792.
46 J. H. Tsai, Y. C. Lai, T. Higashihara, C. J. Lin, M. Ueda and W. C. Chen, *Macromolecules*, 2010, **43**, 6085.
47 L. Leibler, *Macromolecules*, 1980, **13**, 1602.
48 M. W. Matsen and M. Schick, *Phys. Rev. Lett.*, 1994, **72**, 2660.
49 E. J. W. Crossland, M. Nedelcu, C. Ducati, S. Ludwigs, M. A. Hillmyer, U. Steiner and H. J. Snaith, *Nano Lett.*, 2009, **9**, 2813.
50 M. Sommer, S. Huettner and M. Thelakkat, *J. Mater. Chem.*, 2010, **20**, 10788.
51 E. W. Price, Y. Y. Guo, C. W. Wang and M. G. Moffitt, *Langmuir*, 2009, **25**, 6398.
52 J. Ruokolainen, R. Makinen, M. Torkkeli, T. Makela, R. Serimaa, G. ten Brinke and O. Ikkala, *Science*, 1998, **280**, 557.
53 R. D. Groot and T. J. Madden, *J. Chem. Phys.*, 1998, **108**, 8713.
54 Z. J. Guo, G. J. Zhang, F. Qiu, H. D. Zhang, Y. L. Yang and A. C. Shi, *Phys. Rev. Lett.*, 2008, **101**, 028301.
55 A. Sperschneider, M. Hund, H. G. Schoberth, F. H. Schacher, L. Tsarkova, A. H. E. Muller and A. Boker, *ACS Nano*, 2010, **4**, 5609.
56 E. W. Cochran, C. J. Garcia-Cervera and G. H. Fredrickson, *Macromolecules*, 2006, **39**, 2449.
57 I. Botiz and S. B. Darling, *Mater. Today*, 2010, **13**, 42.
58 Y. C. Tseng and S. B. Darling, *Polymers*, 2010, **2**, 470.
59 Y. Z. Yang, F. Qiu, H. D. Zhang and Y. L. Yang, *Polymer*, 2006, **47**, 2205.
60 D. A. Rider, K. A. Cavicchi, L. Vanderark, T. P. Russell and I. Manners, *Macromolecules*, 2007, **40**, 3790.
61 J. I. Lee, S. H. Cho, S. M. Park, J. K. Kim, J. K. Kim, J. W. Yu, Y. C. Kim and T. P. Russell, *Nano Lett.*, 2008, **8**, 2315.
62 J. T. Chen, E. L. Thomas, C. K. Ober and G. P. Mao, *Science*, 1996, **273**, 343.
63 M. Shah and V. Ganesan, *Macromolecules*, 2010, **43**, 543.
64 U. Scherf, A. Gutacker and N. Koenen, *Acc. Chem. Res.*, 2008, **41**, 1086.
65 H. Sirringhaus, *Nat. Mater.*, 2003, **2**, 641.
66 B. D. Olsen and R. A. Segalman, *Macromolecules*, 2005, **38**, 10127.
67 B. D. Olsen and R. A. Segalman, *Macromolecules*, 2007, **40**, 6922.
68 K. M. Coakley and M. D. McGehee, *Chem. Mater.*, 2004, **16**, 4533.
69 Y. F. Tao, B. W. Ma and R. A. Segalman, *Macromolecules*, 2008, **41**, 7152.
70 S. Barrau, T. Heiser, F. Richard, C. Brochon, C. Ngov, K. van de Wetering, G. Hadziioannou, D. V. Anokhin and D. A. Ivanov, *Macromolecules*, 2008, **41**, 2701.
71 J. S. Liu, E. Sheina, T. Kowalewski and R. D. McCullough, *Angew. Chem., Int. Ed.*, 2001, **41**, 329.
72 C. A. Dai, W. C. Yen, Y. H. Lee, C. C. Ho and W. F. Su, *J. Am. Chem. Soc.*, 2007, **129**, 11036.
73 C. C. Ho, Y. H. Lee, C. A. Dai, R. A. Segalman and W. F. Su, *Macromolecules*, 2009, **42**, 4208.
74 H. B. Wang, H. H. Wang, V. S. Urban, K. C. Littrell, P. Thiyagarajan and L. P. Yu, *J. Am. Chem. Soc.*, 2000, **122**, 6855.
75 J. F. Lutz, *Angew. Chem., Int. Ed.*, 2007, **46**, 1018.
76 S. Barth and H. Bassler, *Phys. Rev. Lett.*, 1997, **79**, 4445.

77 T. Q. Nguyen, I. B. Martini, J. Liu and B. J. Schwartz, *J. Phys. Chem. B*, 2000, **104**, 237.
78 P. A. van Hal, M. M. Wienk, J. M. Kroon, W. J. H. Verhees, L. H. Slooff, W. J. H. van Gennip, P. Jonkheijm and R. A. J. Janssen, *Adv. Mater.*, 2003, **15**, 118.
79 T. Kietzke, H. H. Horhold and D. Neher, *Chem. Mater.*, 2005, **17**, 6532.
80 K. T. Early, P. K. Sudeep, T. Emrick and M. D. Barnes, *Nano Lett.*, 2010, **10**, 1754.
81 B. D. Olsen, D. Alcazar, V. Krikorian, M. F. Toney, E. L. Thomas and R. A. Segalman, *Macromolecules*, 2008, **41**, 58.
82 T. Heiser, G. Adamopoulos, M. Brinkmann, U. Giovanella, S. Ould-Saad, C. Brochon, K. van de Wetering and G. Hadziioannou, *Thin Solid Films*, 2006, **511**, 219.
83 B. D. Olsen, X. Gu, A. Hexemer, E. Gann and R. A. Segalman, *Macromolecules*, 2010, **43**, 6531.
84 M. W. Matsen and C. Barrett, *J. Chem. Phys.*, 1998, **109**, 4108.
85 V. Pryamitsyn and V. Ganesan, *J. Chem. Phys.*, 2004, **120**, 5824.
86 S. Nojima, Y. Fukagawa and H. Ikeda, *Macromolecules*, 2009, **42**, 9515.
87 J. K. J. van Duren, X. N. Yang, J. Loos, C. W. T. Bulle-Lieuwma, A. B. Sieval, J. C. Hummelen and R. A. J. Janssen, *Adv. Funct. Mater.*, 2004, **14**, 425.
88 U. Stalmach, B. de Boer, C. Videlot, P. F. van Hutten and G. Hadziioannou, *J. Am. Chem. Soc.*, 2000, **122**, 5464.
89 M. H. van der Veen, B. de Boer, U. Stalmach, K. I. van de wetering and G. Hadziioannou, *Macromolecules*, 2004, **37**, 3673.
90 S. S. Sun, C. Zhang, A. Ledbetter, S. Choi, K. Seo, C. E. Bonner, M. Drees and N. S. Sariciftci, *Appl. Phys. Lett.*, 2007, **90**, 043117.
91 J. Peet, M. L. Senatore, A. J. Heeger and G. C. Bazan, *Adv. Mater.*, 2009, **21**, 1521.
92 R. C. Hiorns, E. Cloulet, E. Ibarboure, A. Khoukh, H. Bejbouji, L. Vignau and H. Cramail, *Macromolecules*, 2010, **43**, 6033.
93 R. S. Loewe, S. M. Khersonsky and R. D. McCullough, *Adv. Mater.*, 1999, **11**, 250.
94 R. D. McCullough, *Adv. Mater.*, 1998, **10**, 93.
95 M. He, J. Ge, M. Fang, F. Qiu and Y. L. Yang, *Polymer*, 2010, **51**, 2236.
96 V. D. Mihailetchi, H. X. Xie, B. de Boer, L. J. A. Koster and P. W. M. Blom, *Adv. Funct. Mater.*, 2006, **16**, 699.
97 Y. Kim, S. Cook, S. M. Tuladhar, S. A. Choulis, J. Nelson, J. R. Durrant, D. D. C. Bradley, M. Giles, I. McCulloch, C. S. Ha and M. Ree, *Nat. Mater.*, 2006, **5**, 197.
98 G. Li, V. Shrotriya, Y. Yao, J. S. Huang and Y. Yang, *J. Mater. Chem.*, 2007, **17**, 3126.
99 A. J. Moule and K. Meerholz, *Adv. Mater.*, 2008, **20**, 240.
100 M. Campoy-Quiles, T. Ferenczi, T. Agostinelli, P. G. Etchegoin, Y. Kim, T. D. Anthopoulos, P. N. Stavrinou, D. D. C. Bradley and J. Nelson, *Nat. Mater.*, 2008, **7**, 158.
101 S. S. van Bavel, E. Sourty, G. de With and J. Loos, *Nano Lett.*, 2009, **9**, 507.
102 M. Dante, C. Yang, B. Walker, F. Wudl and T. Q. Nguyen, *Adv. Mater.*, 2010, **22**, 1835.
103 J. U. Lee, A. Cirpan, T. Emrick, T. P. Russell and W. H. Jo, *J. Mater. Chem.*, 2009, **19**, 1483.
104 J. U. Lee, J. W. Jung, T. Emrick, T. P. Russell and W. H. Jo, *Nanotechnology*, 2010, **21**, 105201.
105 C. Yang, J. K. Lee, A. J. Heeger and F. Wudl, *J. Mater. Chem.*, 2009, **19**, 5416.
106 S. B. Darling, *Energy Environ. Sci.*, 2009, **2**, 1266.
107 I. Botiz and S. B. Darling, *Macromolecules*, 2009, **42**, 8211.
108 A. de Cuendias, R. C. Hiorns, E. Cloutet, L. Vignau and H. Cramail, *Polym. Int.*, 2010, **59**, 1452.
109 Y. Zhang, K. Tajima, K. Hirota and K. Hashimoto, *J. Am. Chem. Soc.*, 2008, **130**, 7812.
110 K. Ohshimizu and M. Ueda, *Macromolecules*, 2008, **41**, 5289.
111 H. B. Wang, M. K. Ng, L. M. Wang, L. P. Yu, B. H. Lin, M. Meron and Y. N. Xiao, *Chem.–Eur. J.*, 2002, **8**, 3246.
112 H. Plank, R. Guntner, U. Scherf and E. J. W. List, *Adv. Funct. Mater.*, 2007, **17**, 1093.
113 Y. Y. Liang, H. B. Wang, S. W. Yuan, Y. G. Lee and L. P. Yu, *J. Mater. Chem.*, 2007, **17**, 2183.
114 Y. S. Sun, T. M. Chung, Y. J. Li, R. M. Ho, B. T. Ko, U. S. Jeng and B. Lotz, *Macromolecules*, 2006, **39**, 5782.
115 M. W. Matsen, *Eur. Phys. J. E*, 2006, **21**, 199.
116 P. T. Wu, G. Q. Ren, C. X. Li, R. Mezzenga and S. A. Jenekhe, *Macromolecules*, 2009, **42**, 2317.
117 A. Yokoyama, A. Kato, R. Miyakoshi and T. Yokozawa, *Macromolecules*, 2008, **41**, 7271.
118 A. Bolognesi, P. Betti, C. Botta, S. Destri, U. Giovanella, J. Moreau, M. Pasini and W. Porzio, *Macromolecules*, 2009, **42**, 1107.
119 U. Scherf, S. Adamczyk, A. Gutacker and N. Koenen, *Macromol. Rapid Commun.*, 2009, **30**, 1059.
120 J. Ge, M. He, F. Qiu and Y. L. Yang, *Macromolecules*, 2010, **43**, 6422.
121 G. Q. Ren, P. T. Wu and S. A. Jenekhe, *Chem. Mater.*, 2010, **22**, 2020.
122 M. He, L. Zhao, J. Wang, W. Han, Y. L. Yang, F. Qiu and Z. Q. Lin, *ACS Nano*, 2010, **4**, 3241.
123 N. Kiriy, E. Jahne, H. J. Adler, M. Schneider, A. Kiriy, G. Gorodyska, S. Minko, D. Jehnichen, P. Simon, A. A. Fokin and M. Stamm, *Nano Lett.*, 2003, **3**, 707.
124 M. Antonietti and S. Forster, *Adv. Mater.*, 2003, **15**, 1323.
125 M. He, W. Han, J. Ge, Y. Y. Yang, F. Qiu and Z. Q. Lin, *Energy Environ. Sci.*, 2011, DOI: 10.1039/c1ee01509e.
126 M. He, W. Han, J. Ge, W. J. Yu, Y. Y. Yang, F. Qiu and Z. Q. Lin, *Nanoscale*, 2011, DOI: 10.1039/c1nr10293a.
127 S. Tatemichi, M. Ichikawa, T. Koyama and Y. Taniguchi, *Appl. Phys. Lett.*, 2006, **89**, 112108.
128 B. A. Jones, A. Facchetti, M. R. Wasielewski and T. J. Marks, *J. Am. Chem. Soc.*, 2007, **129**, 15259.
129 J. H. Oh, S. H. Liu, Z. N. Bao, R. Schmidt and F. Wurthner, *Appl. Phys. Lett.*, 2007, **91**, 212107.
130 Y. F. Tao, B. McCulloch, S. Kim and R. A. Segalman, *Soft Matter*, 2009, **5**, 4219.
131 Q. L. Zhang, A. Cirpan, T. P. Russell and T. Emrick, *Macromolecules*, 2009, **42**, 1079.
132 W. S. Shin, H. H. Jeong, M. K. Kim, S. H. Jin, M. R. Kim, J. K. Lee, J. W. Lee and Y. S. Gal, *J. Mater. Chem.*, 2006, **16**, 384.
133 M. Sommer, S. Huttner, U. Steiner and M. Thelakkat, *Appl. Phys. Lett.*, 2009, **95**, 183308.
134 S. Miyanishi, Y. Zhang, K. Tajima and K. Hashimoto, *Chem. Commun.*, 2010, **46**, 6723.
135 M. Sommer, S. Huttner, S. Wunder and M. Thelakkat, *Adv. Mater.*, 2008, **20**, 2523.
136 P. L. T. Boudreault, A. Najari and M. Leclerc, *Chem. Mater.*, 2011, **23**, 456.

